



Aerosol hygroscopicity over the South-East Atlantic Ocean during the biomass burning season: Part II – Influence of burning conditions on CCN hygroscopicity

Haochi Che^{1,2,a}, Lu Zhang^{2,a}, Michal Segal-Rozenhaimer^{3,a}, Caroline Dang^{3,4}, Paquita Zuidema⁵, Arthur J. Sedlacek III⁶

5 ¹Department of Geosciences, University of Oslo, Oslo, 0315, Norway

²Department of Environmental Science, iClimate, Aarhus University, Roskilde, 4000, Denmark

³Bay Area Environmental Research Institute, NASA Ames Research Center, Moffett Field, CA 94035, USA

⁴NASA Ames Research Center, Moffett Field, CA 94035, USA

⁵Rosenstiel School of Marine and Atmospheric Sciences, University of Miami, Miami, FL 33149, USA

10 ⁶Brookhaven National Laboratory, Upton, NY 11973, USA

^aFormerly at Department of Geophysics, Tel Aviv University, Tel Aviv, 69978, Israel

Corresponding author: Haochi Che (haochi.che@geo.uio.no) and Lu Zhang (luzhang@envs.au.dk)

Abstract

Biomass burning (BB) is an important source of cloud condensation nuclei in the Southeast Atlantic (SEA). The formation of
15 cloud droplets depends on aerosol hygroscopicity (κ), but its variations during the BB season are poorly understood. In this
study, we investigate κ during the 2016 and 2017 BB seasons using 18 months of in situ observations on Ascension Island.
The results show that κ varied monthly, reaching a low in August and increasing from September to October. The mean κ was
0.33 in 2016 and 0.55 in 2017, showing a significant difference. The changes in κ were mainly associated with differences in
the mass fraction of sulfate aerosol. Source attribution showed that about 67% of the sulfate-containing particles originated
20 from BB, suggesting that BB is the main driver of the changes in sulfate aerosol. The ratio of black carbon to excess carbon
monoxide (BC/ Δ CO), used to indicate BB combustion conditions, correlated well with κ and the sulfate mass fraction: higher
ratios (more flaming combustion) reduced the sulfate mass fraction and thus a lower κ . Therefore, the observed lower BC/ Δ CO
ratios in 2017 explain the higher κ values, suggesting less flaming combustion in that year. Meteorological changes in 2017,
including lower wind speeds and higher relative humidity in Africa, may contributed to the altered combustion conditions,
25 explaining the lower BC/ Δ CO and higher κ in 2017. Overall, this study highlights the critical role of BB in understanding the
sulfate budget, aerosol hygroscopicity, and CCN concentration in the marine boundary of the SEA.



1 Introduction

30 The South-East Atlantic Ocean (SEA) is covered by one of Earth's most extensive stratocumulus cloud decks (Wood, 2012). These semi-permanent clouds can result in a significant radiative effect on global climate (Soden and Vecchi, 2011; Wood, 2012). A distinctive feature of these stratocumulus clouds is their interaction with biomass burning (BB) aerosols that are transported from widespread fires in southern Africa from June to October. Although these aerosols substantially impact the underlying stratocumulus cloud deck and the overall radiative balance through aerosol-cloud interactions, the specific effects remain poorly understood, contributing to uncertainties in climate models (Adebiyi and Zuidema, 2016; Che et al., 2021; Gordon et al., 2018; Wilcox, 2012).

A critical aspect of aerosol-cloud interactions involves aerosol particles acting as cloud condensation nuclei (CCN), which facilitate the formation of cloud droplets under supersaturated conditions. Variations in CCN concentrations can significantly impact cloud properties and precipitation patterns (Boucher et al., 2013; Christensen et al., 2020; Lu et al., 2018; Ramanathan et al., 2001; Rosenfeld et al., 2008). The effectiveness of aerosol particles as CCN is mainly determined by their size and hygroscopicity, with the latter characterized by the parameter κ , which is influenced by the chemical composition of aerosols (Petters and Kreidenweis, 2007). Changes in κ can greatly influence cloud droplet formation, especially in the marine boundary layer (MBL) over SEA, where intermediate aerosol concentrations (500-800 cm⁻³) prevail (Kacarab et al., 2020).

BB is a major source of aerosol particles in the SEA, where large quantities of organic aerosol (OA) and black carbon (BC) are emitted into the atmosphere, significantly contributing to CCN concentrations in this region (Che et al., 2022c). The chemical composition of BB aerosol particles is strongly dependent on combustion conditions and the extent of aging of the particles, leading to uncertainties in κ values (Akagi et al., 2012; Hodshire et al., 2019). Laboratory studies have found that freshly emitted BB aerosol particles exhibit a broad range of κ values (from 0.06 to 0.6), but after a few hours of aging, κ converges to approximately 0.2 ± 0.1 (Engelhart et al., 2012). This change in κ with aging is primarily driven by the oxidation of OA and the production of secondary organic aerosols, while the initial variation in κ in fresh BB aerosols is related to the proportion of inorganic components (Engelhart et al., 2012). Additionally, photolysis has been found to significantly reduce OA mass during the weeklong aging of BB aerosols over the SEA, thus affecting their hygroscopicity (Dobracki et al., 2024; Sedlacek et al., 2022). Furthermore, BB aerosols within the SEA boundary layer may undergo cloud processing as they travel through extensive stratocumulus clouds from the free troposphere, which will alter their chemical and physical properties (Che et al., 2022a). Therefore, aerosol hygroscopicity κ can have large variations due to the multiple processes affecting the chemical composition of BB aerosols in the SEA, potentially resulting in substantial uncertainties regarding the aerosol indirect effect.

In addition to BB aerosols, sea-salt particles can significantly affect CCN concentrations in the marine boundary layer over the SEA because of their high κ values (Dedrick et al., 2024; Petters and Kreidenweis, 2007). A study examining collected particles in the SEA found that BB and sea-salt aerosol particles are generally well mixed in the marine boundary layer (Dang et al., 2022). Consequently, the hygroscopicity of aerosols in this region varies with changes in the relative contributions of



BB aerosols and sea salts. While a review suggests that a κ value of $\sim 0.7 \pm 0.2$ is useful as a first approximation for remote ocean environments (Andreae and Rosenfeld, 2008), this value may be too high and unsuitable for the SEA, as the presence of BB aerosols can significantly reduce the overall κ of the mixed aerosols.

65 The single scatter albedo of aerosols observed within the MBL in the SEA showed significant changes throughout the BB season (Zuidema et al., 2018b), which may be driven by variations in BB combustion conditions (Che et al., 2022b; Dobracki et al., 2024). Different combustion conditions can lead to differences in the chemical and physical properties of BB aerosols (Akagi et al., 2012; Zheng et al., 2018), resulting in corresponding differences in the overall κ of aerosols in the MBL during the BB season. However, there have been few studies focusing on the hygroscopicity of aerosols in the MBL layer in the SEA, and most of these studies examine a short time duration (Kacarab et al., 2020; Maßling et al., 2003). Consequently, large
70 uncertainties exist in the overall aerosol hygroscopicity and its variability, affecting cloud properties and the regional climate.

The Layered Atlantic Smoke Interactions with Clouds (LASIC), an 18-month field observation campaign, was conducted from June 1, 2016, to October 31, 2017, on Ascension Island in the SEA to address these uncertainties. The island is located midway between Africa and South America, within the trade wind shallow cumulus regime, and frequently encounters BB aerosol plumes from southern Africa during the BB season (Adebisi and Zuidema, 2016). The continuous observations from LASIC
75 allow for the study of changes in aerosol hygroscopicity during the BB season. Filter samples were collected during a flight aircraft campaign (The CLOUD–Aerosol–Radiation Interaction and Forcing, CLARIFY) near Ascension Island in 2017 to provide more detailed information on aerosol mixing state and chemical components (Dang et al., 2022). In the current study, we use CCN observations from the island to derive the hygroscopicity κ and to analyze its monthly variation during the BB season. Additionally, we use filter samples to investigate the contributions of marine and biomass burning emissions to the
80 overall κ observed on Ascension Island.

2 Method

2.1 In-situ field observations

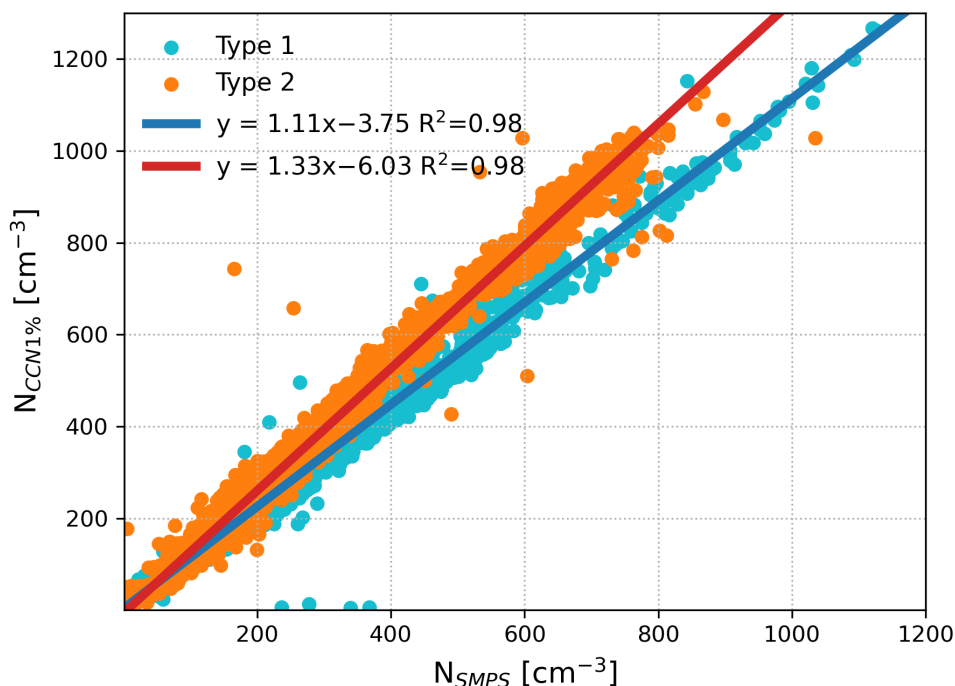
The LASIC campaign was conducted at the Atmospheric Radiation Measurement (ARM) First Mobile Facility (AMF1) site on Ascension Island, located at latitude -7.97° , longitude -14.35° , and an altitude of 341 m. A detailed description of the
85 sampling location and instruments are presented in the campaign report (Zuidema et al., 2018a). Here, we provide a brief overview of the data and instruments utilized in this study. The CCN concentrations at fixed supersaturations were measured using a cloud condensation nuclei counter (CCNC) (Roberts and Nenes, 2005). Aerosol size distributions, ranging from diameters of 10 nm to 500 nm, were measured with a Scanning Mobility Particle Spectrometer (SMPS). Concentrations of aerosol chemical components—including organics, sulfate, nitrate, ammonium, and chloride—were measured using an aerosol
90 chemical speciation monitor (ACSM). Refractive black carbon (BC) was measured using a Single Particle Soot Photometer



(SP2), and carbon monoxide (CO) concentrations were measured using the Los Gatos Model ICOS CO/N₂O/H₂O Analyzer. All instruments were calibrated, and data were converted to standard temperature and pressure conditions. Aerosol chemical composition data is available only for 2017 because of instrumentation issues in 2016. The BC to excess carbon monoxide ratio (BC/ Δ CO) is calculated to analyze the BB conditions, which Δ denotes the difference between observed concentrations and background levels. Note that BC/ Δ CO is unitless, as both BC and CO are converted to the same unit (mass concentration). The background concentrations of CO vary monthly and are determined as the 5th percentiles of measured concentrations in each month. A more detailed discussion about BC/ Δ CO can be found in Che et al. (2022b).

2.2 CCN and SMPS correction

The SMPS size distributions represented as $dN/d\log D$ were first fitted with a bimodal log-normal distribution, and the fitted curve was then extrapolated to obtain the integrated aerosol number concentration (N_{SMPS}) from 3 to 1000 nm. The CCN concentration at 1% supersaturation was generally up to $\sim 30\%$ higher than N_{SMPS} (not shown), suggesting that there were counting errors in one or both instruments. Such errors can lead to an overestimation of the CCN activation rate, which in turn results in an overestimation of the calculated κ . Therefore, it is necessary to correct for these counting errors in CCN and SMPS before calculating κ . A common method to correct for counting errors is to assume that at high supersaturation (e.g., 1%), all aerosol particles activate to form cloud droplets; thus, the N_{SMPS} and the CCN number concentration at 1 % supersaturation ($N_{CCN1\%}$) should be equal. By fitting the $N_{CCN1\%}$ to N_{SMPS} and scaling the CCN or SMPS dataset with the fitted parameters, one can account for counting errors. However, this assumption may overestimate CCN concentration, particularly in situations with a large number of aerosol particles in the nucleation mode. For instance, according to the κ -Köhler equation, the activation of a 20 nm particle at 1% supersaturation requires a κ value of approximately 2.24, which is unrealistically high given that most aerosols have hygroscopicity values less than 1 (Petters and Kreidenweis, 2007). During the LASIC campaign, the aerosol number distribution frequently exhibited a bimodal mode, with the smaller mode having a mode diameter of approximately 40 nm (Dobracki et al., 2024). This indicates a high fraction of small aerosol particles (below 40 nm) observed on Ascension Island. Therefore, using the aforementioned approach to correct for counting errors in CCN and SMPS would likely result in an overestimated κ .



115

Figure 1. Correlations between the CCN concentration measured at 1% supersaturation and the integrated aerosol concentration from the SMPS. Two distinct correlations were identified in the data using the K-means clustering method, indicated by light blue and orange points. Type 1 (light blue) includes data from June, July, September, and October of 2016, while Type 2 (orange) includes data from August 2016 and June to October 2017. The blue and red lines represent linear regressions fitted to each correlation type, respectively.

120

Here we propose a modified method to correct for CCN and SMPS counting errors by assuming only a fraction of particles can be activated at 1% supersaturation. The key step is to determine the critical activation diameter of CCN at this supersaturation. We assume that the aerosol particles observed at the island are a mixture of highly aged biomass burning (BB) aerosols and sea-salt aerosols, with the hygroscopicity of particles in the 20–35 nm size range being approximately 0.6—similar to that of sulfate aerosols. Therefore, we infer a critical activation diameter of 31 nm at 1% supersaturation. We then compared $N_{CCN1\%}$ with the integrated aerosol concentration $N_{SMPS_{31}}$ from 31 to 1000 nm based on SMPS observations. Although our modified method mitigates the risk of overestimating κ , it may still result in a slight overestimation. This is because smaller particles generally have a higher organic fraction and thus lower hygroscopicity than 0.6, implying that the critical diameter at 1% supersaturation should be greater than 31 nm.

130



Applying our modified approach, we observed two types of relationships between $N_{CCN1\%}$ and $N_{SMPS_{31}}$ during the BB seasons in 2016 and 2017. To quantitatively categorize and separate the data, we used K-means clustering, with the results shown in Figure 1. Type 1 includes observations from the 2016 BB season, excluding August, while Type 2 includes observations from the 2017 BB season and August 2016. Both types exhibit strong linear relationships with $R^2 \sim 0.98$. However, the reason for these two distinct linear relationships in $N_{CCN1\%}$ and $N_{SMPS_{31}}$ remains unclear. After successfully establishing the fitting equations for $N_{CCN1\%}$ and $N_{SMPS_{31}}$, we applied the respective equations to each identified type, thereby scaling the CCN data accordingly to account for the counting errors.

2.2 Calculation of κ

The aerosol hygroscopicity κ in our study was calculated using SMPS and the corrected CCN data through the following procedure. First, the aerosol size distribution from the SMPS was first fitted to a bimodal log-normal distribution. Starting with a particle diameter $D = 31$ nm, we extrapolated this fitted size distribution and integrated it from D to 1000 nm. When the integrated aerosol number concentration matches the observed CCN concentration, the current particle diameter D is considered to be the critical diameter D_c . If there was no match, we continued increasing D by 1 nm and repeated the steps until a match was found. Once D_c is identified, the hygroscopicity parameter κ can be calculated using the following equation (Eq. 1):

$$\kappa = \frac{4A^3}{27D_c^3 \ln^2(S_c + 1)} \quad (1)$$

where $A = \frac{4M_w\sigma_{s/a}}{RT\rho_w}$, M_w is the molecular weight of water, $\sigma_{s/a}$ is the surface tension of the droplet/air interface and equals to 0.072 J m⁻², R is the universal gas constant, ρ_w is the density of water, T is the temperature and equals to 298 K, and S_c is the supersaturation in the unit of %. Because cloud supersaturation in this region is generally low and mostly below 0.1% (Che et al., 2021), we use the CCN concentration measured at 0.1% supersaturation to estimate κ in this study. However, the κ calculated by this method may still be overestimated, as discussed in the previous section.

2.3 Filter samples

Filter samples were collected using Facility for Airborne Atmospheric Measurements (FAAM)'s filter systems (Sanchez-Marroquin et al., 2019) on the UK's Bae-146 aircraft near Ascension Island in August, 2017. Samples were deposited on Paella TEM grids and analyzed with a JEOL™ JEM-2010F FEG-TEM equipped with a ThermoNoran™ energy-dispersive X-ray detector (EDX) at Tel-Aviv University. There were 17 samples collected near the island, but only 6 taken inside the marine boundary layer (MBL) were used for further analysis in this study. A detailed description of each sample is provided by Dang et al. (2022). A total of 231 particles were analyzed, and elemental mass fractions for individual particles were determined through EDX analysis. Based on back trajectory analyses, filters collected in the MBL were evenly mixed between BB and



160 marine sources, ensuring a representative mix of aerosol sources in the study. Table 1 lists the elements analyzed, along with the mean and standard deviation of the mass fractions for all 231 particles examined.

Table 1. Elements analyzed and their mean and standard deviation of mass fractions for 231 particles.

Elements	Particle number	Mean mass fraction (%)	Mass fraction std (%)
Al	231	0.270736	1.238378
C	231	75.948182	21.117492
Ca	231	0.327576	1.810890
Cl	231	2.174113	6.294387
Co	231	0.005065	0.067790
Cr	231	0.206494	2.794100
F	231	0.016883	0.256601
Fe	231	1.024805	7.862684
K	231	1.746364	3.642440
Mg	231	0.023203	0.204436
N	231	3.353593	7.991303
Na	231	2.195022	4.425461
Ni	231	0.010779	0.163830
O	231	8.925238	8.243104
P	231	0.026970	0.197371
S	231	0.734329	1.765918
Si	231	0.845498	2.288163

2.4 Meteorological data

165 Monthly mean winds at a height of 10 meters above the surface, and air relative humidity at 2 meters above the surface over Africa and the SEA during the BB season for the years 2016 and 2017 were analyzed in this study using data from the ERA5 reanalysis dataset, the fifth-generation reanalysis of the global climate and weather, produced by the European Centre for Medium-Range Weather Forecasts (ECMWF) (Hersbach et al., 2020). The dataset has a horizontal resolution of $0.25^\circ \times 0.25^\circ$.

3 Results

170 3.1 Variation of aerosol hygroscopicity and chemical composition

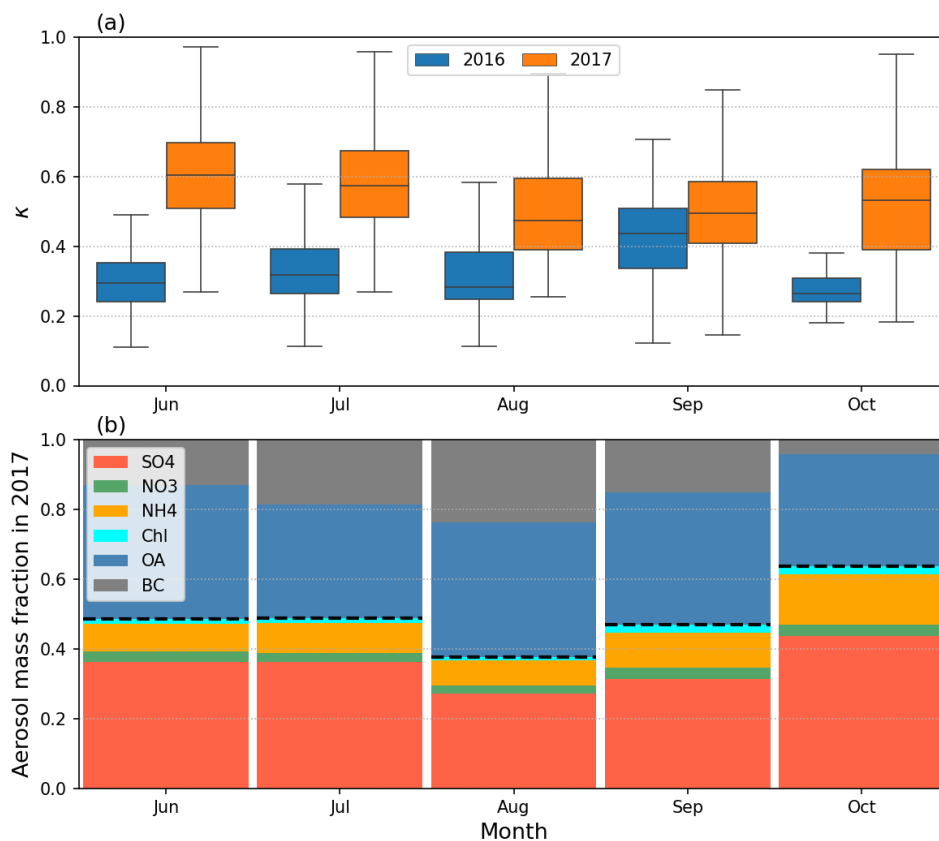


Figure 2. (a) Monthly percentiles (10%, 25%, 50%, 75%, and 90%) of κ calculated at 0.1% supersaturation during the BB seasons of 2016 and 2017. (b) Monthly mean aerosol chemical mass fractions measured by ACSM and SP2 during the 2017 BB season. The black dashed line in (b) represents the separation between inorganic and organic fractions of the aerosol components.

175

The hygroscopicity parameter κ exhibits considerable monthly differences throughout the biomass-burning season, with noticeable differences between the years 2016 and 2017 (Figure 2a). The monthly changes in κ align closely with the patterns observed in aerosol absorption coefficients, characterized by a decline from July to a minimum in August, followed by an increase in September and October (Zuidema et al., 2018). This trend underscores the significant influence of biomass combustion on the hygroscopic properties of marine boundary layer aerosols in the SEA. The monthly values of κ in 2016 ranged from 0.2 to 0.65, with a mean value of 0.33. In contrast, the monthly values in 2017 ranged from 0.3 to 0.78, with a mean of 0.55. According to Andreae and Rosenfeld (2008), $\kappa = 0.7 \pm 0.2$ serves as a typical value for marine aerosols, and

180



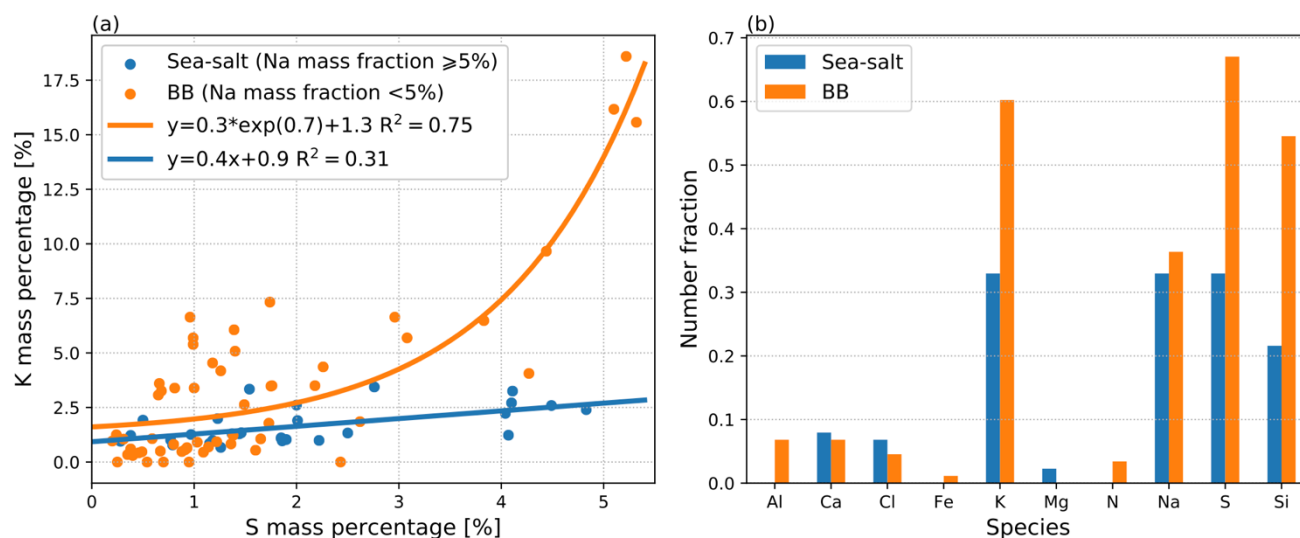
185 Schulze et al. (2020) reported κ values around 0.7 for remote marine regions in the Pacific. The significantly lower κ values observed in this study suggest a strong influence of African BB on the SEA boundary layer, deviating from the characteristics of a typical remote marine environment during the BB season. This conclusion is supported by the ORACLES (ObseRvations of Aerosols above CLouds and their intEractionS) 2017 flight campaign over the SEA (Redemann et al., 2021), which reported average κ values for marine boundary layer aerosols ranging from 0.2 to 0.4 (Kacarab et al., 2020).

190 The distinct difference in κ values between 2016 and 2017 likely reflects changes in aerosol chemical composition between these two years, given that the magnitude of κ is largely influenced by the chemical components of the aerosols. This is supported by Figure 2(b), which presents the monthly mean mass fractions of aerosol compositions during the BB season in 2017. As shown, the mean κ values generally align with the dashed line, which represents the fraction of inorganic components. In general, inorganic aerosol components exhibit higher κ values due to their higher ability to uptake water vapor (Petters and Kreidenweis, 2007). Consequently, the lower κ values observed during the 2016 BB season might be attributed to a reduction in inorganic aerosol components and/or an increase in the organic aerosols compared to 2017. These findings suggest
195 substantial changes in the marine boundary layer aerosol chemical properties in SEA between 2016 and 2017, despite the same general sources of aerosols—primarily BB and sea salt. Additionally, variations in the hygroscopicity of OA between the two years might also contribute to the differences in κ . However, since the κ values for OA are generally low (Pöhlker et al., 2023; Zhang et al., 2023), such changes may not fully account for the overall lower κ values observed in 2016.

200 For the inorganic components, a plausible explanation for the observed differences in κ between 2016 and 2017 could be changes in sulfate mass fraction. As illustrated in Figure 2(b), sulfate aerosols constitute the primary inorganic component, accounting for approximately 35% of the total aerosol mass and around 71% of the inorganic aerosol mass on average during BB season in 2017. The ratio of sulfate to BC and OA in 2017 aligns with the monthly changes in κ (Figure S1, supplementary), confirming that changes in the sulfate mass fraction may explain the differences in κ . The mass fraction of sulfate also exhibits the largest monthly variation in 2017 among all species, ranging from approximately 27% to 44%. Given that sulfate aerosols
205 have a relatively high κ value of ~ 0.6 (Petters and Kreidenweis, 2007), changes in sulfate mass fraction may significantly affect the overall κ observed on the island.



3.2 Sources of sulfate aerosols



210 Figure 3. (a) Mass percentage of sulfate and potassium from different potential sources of aerosols, and (b) number fraction of
215 elements in sulfate-bearing particles. Particles from BB and sea salt are differentiated by the sodium mass fraction; blue
represents sea salt particles, and orange represents BB particles. The lines in (a) represent the fitted correlations, with the
corresponding equation and R^2 value displayed in the figure legend.

Sulfate aerosols observed at Ascension Island likely originate from three different sources: BB emissions, sea salt, and new
215 particle formation (Che et al., 2022c). However, the latter mostly contributes to small particles, which have a limited effect on
the variations in sulfate mass. Therefore, it is likely that changes in biomass burning emissions and sea salt are the main drivers
for the variations in sulfate. In this section, we discuss the primary sources of sulfate to further investigate the reasons behind
the monthly changes in sulfate mass fraction and the changes in κ between 2016 and 2017. We evaluate this by examining the
results from the single-particle filter analysis done by Dang et al. (2022).

220 A potential way to distinguish the contributions of sea salt and BB to sulfate is by using specific tracers for these sources.
Potassium (K) is commonly considered a tracer of BB emissions, while sodium (Na) is predominantly found in sea salt
(Seinfeld and Pandis, 2016). Although Na was also presented in BB plumes over the SEA, it was in lower concentrations and
likely accounted for a smaller weight percentage in individual BB aerosols when analyzed by Energy Dispersive X-ray
Spectroscopy (EDX) (Dang et al., 2022). Therefore, we selected K and Na as tracers for BB aerosols and sea salt, respectively,
225 and made a simple distinction of the sulfate sources based on the concentrations of these tracers.

In Figure 3, a Na mass fraction threshold of 5% has been set to distinguish between the two sulfate sources. This value has
been determined iteratively to allow the separation of the two sources, demonstrating a clear distinction in the correlation



between sulfate and K for each source, as shown in the figure. When the Na mass percentage exceeds 5%, we consider sea salt to be the predominant aerosol source; conversely, when it is below 5%, BB aerosols are considered dominant. As shown in
230 Figure 3(a), K and sulfate exhibit a strong exponential relationship in aerosols when BB is the dominant source, which may
be because the excess K is bonded with nitrates (Dang et al., 2022). This suggests that an increase in BB aerosols can
significantly elevate the proportion of sulfate. For aerosols where sea salt is the main source (blue markers in Figure 3a), there
is no evident relationship between sulfate and K, resulting in a near-zero slope in the fitted line. Both correlations have p-
values lower than 0.05, indicating statistical significance. Therefore, these distinct correlations confirm that the method for
235 distinguishing sulfate origins is reliable and successful in providing a general indication of the dominant source.

Using this classification method, all sulfate-bearing particles sampled within the boundary layer near Ascension Island were
categorized and quantified, as presented in Figure 3(b). Both K and Na are present in aerosol particles from both sources, with
number fractions exceeding 30%. This is because the observed BB aerosols are well-mixed after weeklong aging and
transportation (Che et al., 2022a), aligning with the results from single-particle analysis by Dang et al. (2022) in this region.
240 Nevertheless, K remains predominantly concentrated in BB-origin aerosols. While the Na number count in the two sources is
not significantly different, their mass fractions do differ, with a higher mass fraction of Na originating from sea salt (Figure
3a). The results indicate that BB is the main source of observed sulfate, with approximately 67% of sulfate-bearing particles
originating from BB. Sea salt may contribute the remaining 33% of sulfate, roughly half of the BB contribution. Therefore, it
is likely that variations in BB emissions are the major contributors to the monthly differences in sulfate mass fraction, as well
245 as to the differences in observed κ between 2016 and 2017.

3.3 Effect of BB conditions on aerosol hygroscopicity

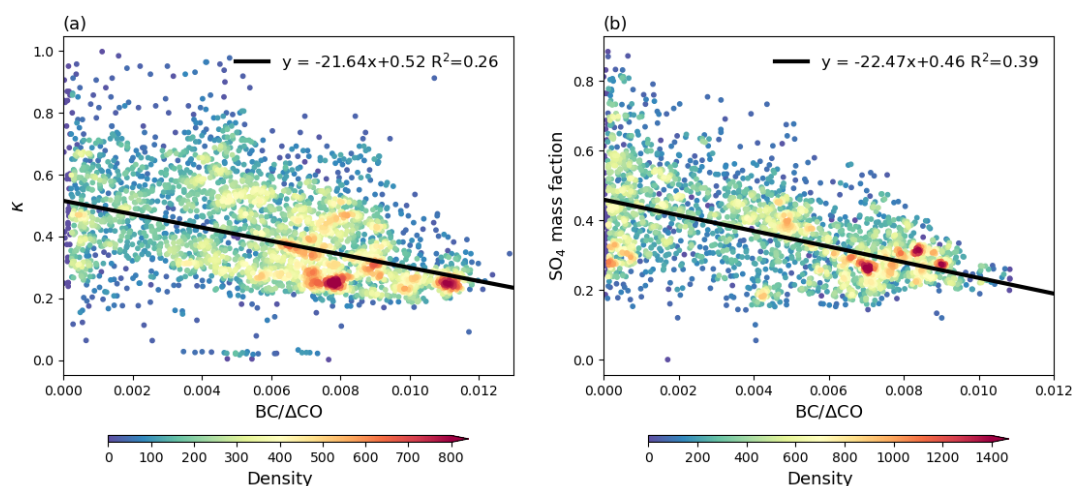


Figure 4. Relationships of BC/ΔCO with (a) κ calculated at 0.1% supersaturation and, (b) sulfate mass fraction. The black lines represent linear regressions, with the corresponding equations displayed in the legend. The color scale indicates the data density,



250 which is the count of the data in the gridded 50x50 bins of the data range. Note that panel (a) includes data from both the 2016 and 2017 BB seasons, whereas panel (b) only includes data from the 2017 BB season.

From the previous section, we found that BB is the dominant source of sulfate. Here, we further analyze how BB influences the sulfate mass fraction, with the first step being to quantify the burning conditions of the biomass. A recent study on LASIC
255 aerosols (Che et al., 2022b) found that the seasonal variation in the aerosol optical properties is affected by BB combustion conditions. These conditions can be approximated by $BC/\Delta CO$, with higher $BC/\Delta CO$ indicating more flaming combustion, and Δ denotes the difference between observed concentrations and background levels. The value of $BC/\Delta CO$ shows a strong linear correlation with modified combustion efficiency (MCE) for freshly emitted BB aerosols, establishing 0.004 as the
260 threshold for distinguishing between flaming and smoldering-dominated combustion in freshly emitted BB aerosols (Che et al., 2022b). For the highly aged aerosols observed on Ascension Island, they estimated that the threshold of $BC/\Delta CO$ is approximately 0.003. When $BC/\Delta CO < 0.003$, the BB aerosols observed are considered to be emitted mainly from smoldering combustion; conversely, when $BC/\Delta CO > 0.003$, they are mainly from flaming combustion.

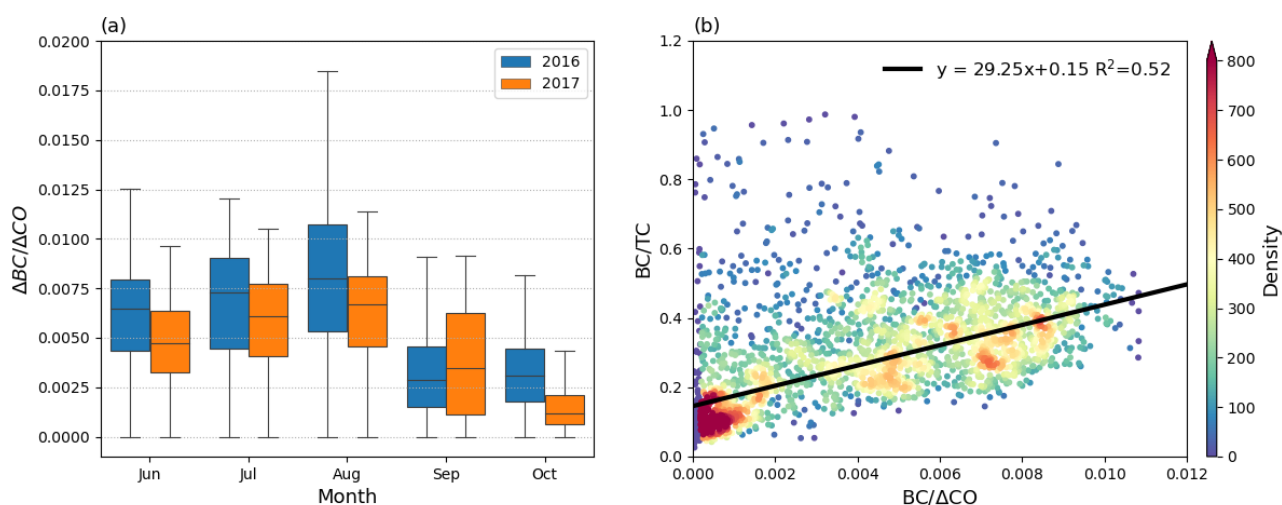
The relationship between $BC/\Delta CO$ and κ is shown in Figure 4(a). The κ generally shows a decreasing trend with increasing $BC/\Delta CO$, confirming that BB combustion conditions affect the aerosol hygroscopicity observed at Ascension Island. As
265 $BC/\Delta CO$ increases, indicating the BB becomes more flaming-dominated, there is a higher emission of BC (Conny and Slater, 2002). Freshly emitted BC particles are insoluble and can significantly reduce aerosol hygroscopicity. However, BC particles observed at Ascension Island, which went through weeklong aging during their transport, became coated with soluble materials (Che et al., 2022b). Such coating can mitigate the reduction in κ due to BC particles, aligning with field observations that show
270 no significant difference in κ between coated BC particles and BC-free particles (Ohata et al., 2016). Therefore, the changes in κ due to $BC/\Delta CO$ are likely driven by changes in the fraction of inorganic and organic components resulting from different burning conditions.

This can be confirmed by Figure 4(b), which shows that the sulfate mass fraction is well correlated with $BC/\Delta CO$, indicating that combustion conditions can influence the sulfate mass fraction in BB aerosols. The correlation is particularly evident when
275 $BC/\Delta CO > 0.003$, as shown by the apparent decrease in sulfate mass fraction with increasing $BC/\Delta CO$. This suggests that in flaming-dominated combustion, the sulfate mass fraction decreases as the combustion becomes more flaming. Figure S2 illustrates that both the mass concentration of sulfate and the total aerosol particles increase with $BC/\Delta CO$, implying that the decreasing sulfate mass fraction with higher $BC/\Delta CO$ is not due to a reduction in sulfate mass. Instead, it results from a more significant increase in the mass of species such as BC and OA, which decreases the relative fraction of sulfate. When $BC/\Delta CO < 0.003$, indicating smoldering-dominated combustion, the correlation between the sulfate mass fraction and $BC/\Delta CO$ weakens
280 due to more scattered data. The aerosol mass is also relatively low when $BC/\Delta CO < 0.003$, suggesting relatively clean conditions. As a result, the contribution of sulfate from other sources, such as sea salt, becomes more prominent, leading to a



weaker correlation between sulfate mass fraction and BB combustion conditions. This is supported by a study that showed different aerosol size distributions when the BB plume mixes with clean air (Dobracki et al., 2024).

3.4 Changes in BB conditions



285

Figure 5. (a) Monthly percentiles (10%, 25%, 50%, 75%, and 90%) of BC/ΔCO presented as box-and-whisker plots for the BB seasons of 2016 (blue) and 2017 (orange). (b) Relationship between BC/ΔCO and the BC to TC (total carbon) mass ratio during the BB season in 2017. The color scale in (b) indicates data density, represented as the count of data points within gridded 50x50 bins of the data range.

290 The monthly distribution of BC/ΔCO during the BB seasons of 2016 and 2017 is illustrated in Figure 5(a). Given that BC/ΔCO is negatively correlated with both the sulfate aerosol mass fraction and κ , the monthly variations in BC/ΔCO suggest changes in BB conditions that may account for the observed aerosol hygroscopicity changes. From June to August 2017, an increase in BC/ΔCO coincided with a decrease in κ and sulfate mass fraction. Conversely, the decrease in BC/ΔCO from August to October 2017 was accompanied by an increase in both sulfate mass fraction and κ . In 2016, considerable fluctuations in
295 BC/ΔCO, demonstrated by the large range between the 10th and 90th percentiles in each month, preclude the identification of a clear pattern between the monthly mean κ and BC/ΔCO. However, the highest average κ in 2016 was found in September, coinciding with the lowest average BC/ΔCO for that month, suggesting that combustion conditions still explain the observed changes in κ for that year.

The median BC/ΔCO ranges from 0.0029 to 0.008 in 2016 and from 0.0012 to 0.0067 in 2017. According to the estimated
300 threshold of ~ 0.003 for distinguishing BB aerosols from flaming and smoldering emissions, most of the BB aerosols observed at Ascension Island originate from flaming combustion, with only September and October showing a higher proportion of

aerosols from smoldering combustion. As discussed earlier, when the combustion becomes smoldering-dominated, the concentration of BB aerosols reaching the island is relatively low. Consequently, the influence of marine-origin aerosols on κ becomes more important, making the relation between $BC/\Delta CO$ and κ less clear in those months.

305 Comparing $BC/\Delta CO$ values across the two years, BB fires in 2017 generally exhibited lower $BC/\Delta CO$ values, indicating less
flaming combustion. This finding is consistent with the higher κ values observed in 2017 compared to 2016. Since $BC/\Delta CO$
affects κ by influencing the sulfate aerosol mass fraction, we infer that the variations in burning conditions between 2016 and
2017 resulted in differences in sulfate aerosol mass fractions. Specifically, the higher $BC/\Delta CO$ values in 2016 suggest a
generally lower fraction of sulfate aerosols in each month during the BB season, leading to lower aerosol hygroscopicity
310 compared to 2017.

Since the observed BB aerosols are highly aged, the value of $BC/\Delta CO$ can also be affected by removal processes such as wet
and dry deposition during the transport of the BB plume. Wet removal primarily occurs through interaction with cloud droplets
and precipitation, which can reduce the $BC/\Delta CO$ ratio. Che et al. (2022b) analyzed the cloud fraction and precipitation during
the BB season in 2016 and 2017 and found no significant difference between these two years. This suggests that the major
315 difference in κ between 2016 and 2017 is not due to changes in wet deposition. For dry deposition, it is mainly influenced by
the transport pathway and distance. However, similar transport pathways and distances were found for both years (Che et al.,
2022b), indicating that dry deposition is also not responsible for the changes in $BC/\Delta CO$ observed between these two years.
Therefore, the changes in $BC/\Delta CO$ may be primarily attributed to changes in burning conditions. This conclusion is supported
by Figure 5(b), which shows that the ratio of BC to total carbon (TC, which is the sum of OA and BC) increases with $BC/\Delta CO$.
320 This finding is consistent with previous studies, such as Conny and Slater (2002), which reported that flaming combustion
tends to have a high BC/TC ratio, whereas the BC/TC ratio for smoldering combustion is generally very low. Therefore, we
conclude that aerosol hygroscopicity is primarily influenced by the combustion conditions of the biomass. However, sea salt
may have some impact especially when burning becomes more smoldering, corresponding to the low concentrations of BB
aerosols observed at Ascension Island.

325

3.5 Changes in organic aerosol hygroscopicity

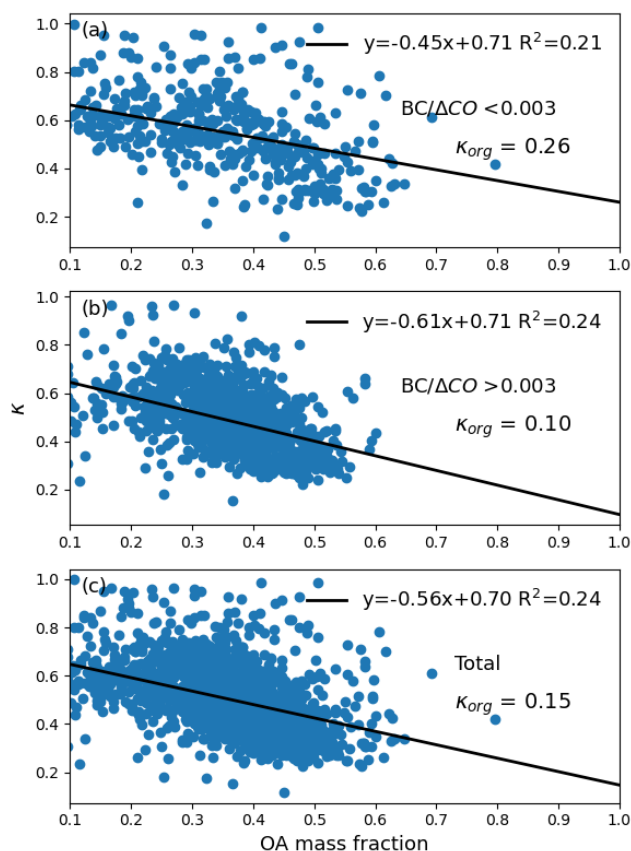


Figure 6. Correlation between the observed hygroscopicity κ at 0.1% supersaturation and the organic aerosol (OA) mass fraction during different combustion conditions: (a) smoldering-dominated fires, (b) flaming-dominated fires, and (c) the entire BB season of 2017.

As discussed earlier, the changes in κ between 2016 and 2017 may stem from two main aspects: changes in the inorganic mass fraction and potential changes in the hygroscopicity of organic aerosols (κ_{org}). While the latter may not fully account for the total variation in κ , it may still contribute to the observed differences. In this section, we discuss κ_{org} observed during the BB season of 2017. As illustrated in Figure 6, κ is linearly correlated with the mass fraction of organic aerosols. Although κ , by definition, depends on the chemical composition of aerosols and the volume fraction of each component, using the mass fraction provides a simple yet reliable estimation, and is widely used in observations and CCN predictions (Chang et al., 2010; Che et al., 2017; Pöhlker et al., 2023; Rose et al., 2010, 2011). Based on the established linear relationship between the OA mass fraction and overall κ , we can infer κ_{org} by extrapolating the linear regression, assuming the mass fraction of OA is 1.



340 From the figure, κ_{org} varies for OA produced by different combustion conditions. When $BC/\Delta CO < 0.003$, κ_{org} is higher, with
a mean value of ~ 0.26 (Figure 6a), indicating that smoldering-dominated combustion can result in more hygroscopic aged OA.
Under flaming-dominated combustion (i.e., $BC/\Delta CO > 0.003$, figure 6b), the average κ_{org} is ~ 0.1 , suggesting that OA from
flaming BB fires is less hygroscopic. The variation in κ_{org} may be related to the degree of oxidation of OA under different
combustion types, as the hygroscopicity of OA generally increases with O:C ratios, although this relationship is not linear
345 (Han et al., 2021). Thus, the higher κ_{org} associated with low $BC/\Delta CO$ may suggest that OA from smoldering combustion is
more oxidized. However, since the aerosols observed at Ascension Island undergo a weeklong period of aging, both oxidation
and photolysis can significantly affect the chemical and physical properties of OA (Che et al., 2022a). Consequently, the
mechanisms leading to changes in κ_{org} are complex and require further investigation. Weimer et al. (2008) showed that mass
spectra during the smoldering phase are dominated by oxygenated species, resembling fulvic acid, which is used as a model
350 compound for highly oxidized aerosols. This suggests that smoldering combustion may produce highly hygroscopic OA. In
addition to these potentially highly hygroscopic OAs, the long period of aging likely contributes further to the oxidation of
OA from smoldering combustion. This is because smoldering combustion generates more OA and volatile organic gases,
which can form secondary OA through further oxidation (Haslett et al., 2018). Therefore, given the higher $BC/\Delta CO$ in 2016,
 κ_{org} in 2016 is likely lower than in 2017, contributing to the generally lower aerosol hygroscopicity observed in 2016.

355 Figure 6(c) shows the averaged OA κ_{org} during the entire BB season of 2017. The observed mean κ_{org} throughout this period
is approximately 0.15. This finding aligns with the value of 0.11 reported from subsaturated conditions observed during aircraft
measurements in the same region during the BB season in 2016 and 2018 (Zhang et al., 2023). It also matches closely with a
field study at a remote marine site in the eastern Mediterranean, which experienced remotely transported BB aerosols during
their observation, and found κ_{org} to be approximately 0.158 (Bougiatioti et al., 2009). Overall, the observed OA hygroscopicity
360 at Ascension Island falls within the range of highly aged (oxidized) OA hygroscopicity described by Petters and Kreidenweis
(2007). This suggests that the BB aerosols observed at Ascension Island are highly aged and thus have a higher hygroscopicity
than freshly emitted aerosols near the continent. As these highly aged BB aerosols are transported over the ocean, where
abundant water vapor and high cloud fractions prevail, changes in aerosol hygroscopicity become crucial in influencing cloud
properties.

365

370

3.6 Potential changes in burning conditions and sea-salt emissions

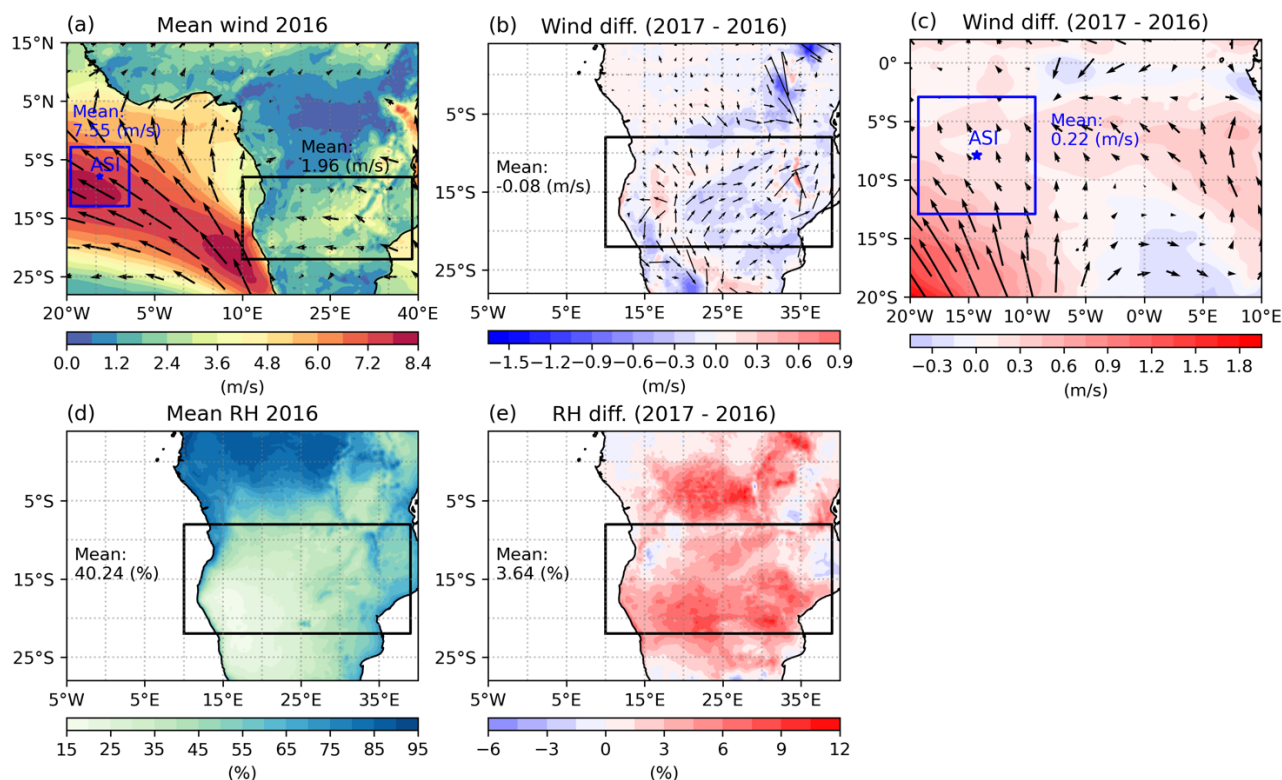


Figure 7. June-October mean surface wind in (a) 2016, and the difference between 2017 and 2016 over the (b) African continent and (c) Ascension Island. (d) Mean relative humidity (RH) for the same period in 2016, and (e) the difference between 2017 and 2016 over Africa. The black boxes indicate areas with the majority of BB combustion events, while the blue boxes represent the region centered on Ascension Island, extending ± 4 degrees in latitude and longitude. The means within the black and blue box regions are displayed with the corresponding colors. Note: In (d-e), the unit (%) is the unit of RH, not the relative change in percentage.

375 In this section, we discuss the potential reasons behind the changes in BB conditions between 2016 and 2017, as well as the potential contribution of sea salt. Several factors can influence BB conditions, such as the water content in the fuel, humidity, and wind speed. Here we focus primarily on wind speed and relative humidity RH. Wind speed can directly affect the oxygen supply, which is closely related to combustion conditions. It also can impact sea salt emissions. RH primarily affects the burning conditions by influencing the moisture level.



385 The mean wind field is shown in Figure 7(a). The dominant wind over both the land and the island was westerly. During the
BB season in 2016, the mean wind speed was approximately 7.6 m/s around Ascension Island and around 2 m/s over the BB
areas on land (excluding the ocean). In 2017, there was a slight reduction in wind speed (0.08 m/s) over the BB burning region
on land (Figure 7b), accompanied by an increase in easterly winds, which are opposite to the plume transport pathway. Studies
have shown that wind can increase oxygen supply and lead to more flaming combustion, although strong winds can also reduce
390 flaming by increasing cooling (Santoso et al., 2019). Therefore, the slight reduction in wind speed during the 2017 (around
4%) BB season may have resulted in a reduction in oxygen supply to the BB combustion, causing it to become less flaming.
This change is consistent with the variation in $BC/\Delta CO$. Therefore, it is likely that the change in wind speed contributed to the
difference in $BC/\Delta CO$ between 2016 and 2017.

Sea-salt aerosols have a strong relationship with surface wind, and a linear correlation is observed between wind speed and
395 sea salt aerosol production rate (Priyith et al., 2014). In the blue area in Figure 7(c), centered on Ascension Island and extending
4 degrees in latitude and longitude, mean surface wind speeds increased by an average of 0.22 m/s (approximately 3%) during
the 2017 BB season. The mean wind around the island became more westerly, with an increase in winds flowing from the
southern Atlantic towards the island, potentially bringing more sea-salt aerosols to the island. As a result, the sea-salt aerosols
observed during the 2017 BB season may have increased. Since sea-salt aerosols are rich in highly hygroscopic compounds
400 such as NaCl, this potential increase in sea-salt aerosols could result in the observed increase in aerosol hygroscopicity on the
island.

The mean RH during the 2016 BB season over the land is shown in Figure 7(d). The average RH over the BB region was
approximately 40.2% that year, indicating relatively dry conditions that favor flaming combustion. In 2017, the mean RH over
the BB region increased to 43.9%, showing a relative increase of about 9 % from the previous year (Figure 7e). Although the
405 mean RH in 2017 still represents relatively dry conditions, the increased RH may reduce the extent of flaming combustion and
favor smoldering fires by supplying more water vapor. Therefore, it is likely that the change in RH is another reason behind
the difference in $BC/\Delta CO$ between 2016 and 2017.

Overall, during the BB season, there was a slight decrease in surface wind speed in the major BB region over the African
continent in 2017, accompanied by an increase in RH in that region, which favors less flaming combustion. Meanwhile, the
410 sea surface wind speed around Ascension Island increased in 2017. These changes are likely to have contributed to the higher
observed κ in 2017. The decreased wind speed and increased RH over the African continent may have resulted in a lower
 $BC/\Delta CO$, leading to a higher fraction of sulfate. Additionally, the increased sea surface wind speed around the island could
bring in highly hygroscopic species such as NaCl. These results suggest the potential influence of meteorological conditions
on the aerosol hygroscopicity observed on the island.



415 4 Conclusion and discussion

From 1 June 2016 to 31 October 2017, an *in-situ* observation field campaign was conducted on Ascension Island. In this study, we calculated the aerosol hygroscopicity parameter κ using CCN and aerosol size distribution data from the campaign to investigate the aerosol hygroscopicity during the BB season (June-October) in 2016 and 2017.

The results show that κ exhibits significant monthly changes throughout the BB season, with the lowest values observed in August and an increase from September to October. Around 90% of κ values range from 0.21 to 0.74, with most values being lower than the generally used κ value (0.7 ± 0.2) for marine aerosols, indicating the strong influence of BB in the marine boundary layer in the SEA. There is also a noticeable difference in κ values between the BB seasons of 2016 and 2017, with a mean κ of approximately 0.33 in 2016 and about 0.55 in 2017. This significant difference suggests that aerosols in 2017 became more hygroscopic and easier to activate as cloud droplets at the same supersaturation.

The alignment of monthly mean κ values with the fraction of inorganic components suggests that changes in κ reflect changes in aerosol chemical composition. Specifically, the lower κ values in 2016 can be attributed to a reduction in inorganic components and an increase in the organic fraction. Sulfate aerosols, the primary inorganic component, accounted for approximately 35% of the total aerosol mass and around 71% of the inorganic aerosol mass in 2017, with monthly variations ranging from 27% to 44%. Due to the high κ value of sulfate (~ 0.6), changes in sulfate levels are likely a significant factor contributing to the differences in κ .

To understand the source and variations of sulfate aerosols, a simple source attribution was performed using filter samples collected near the island. The results indicated approximately 67% of sulfate-bearing particles originated from BB emissions, while the remaining 33% came from sea salt. This suggests that changes in BB emissions are likely the primary drivers behind the monthly differences in sulfate mass fraction and the observed differences in κ values between 2016 and 2017. To further investigate how BB emissions influence sulfate mass fraction, we quantified the burning conditions using the BC/ Δ CO ratio, where a higher ratio indicates more flaming combustion. A threshold of 0.003 for BC/ Δ CO was established to differentiate between smoldering and flaming-dominated combustion for the highly aged aerosols observed on the island. The value of BC/ Δ CO shows a negative linear correlation with both κ and sulfate mass fraction, indicating that as biomass combustion becomes more flaming, both the sulfate mass fraction and κ value generally decrease. This decrease is attributed to a more significant increase in the mass of species like BC and OA, which reduces the relative fraction of sulfate. Comparing the BC/ Δ CO ratios during the BB season between 2016 and 2017 shows that the ratio was generally lower each month in 2017, implying less flaming combustion that year. This finding is consistent with the higher κ values observed in 2017. Therefore, it is likely that the significant differences in aerosol hygroscopicity between 2016 and 2017 are due to variations in biomass combustion conditions, which resulted in changes in aerosol chemical composition.



445 The hygroscopicity of organic aerosols κ_{org} was analyzed under different BB conditions, revealing that κ_{org} varies based on the combustion conditions. The mean κ_{org} for the entire BB season is 0.15. Higher κ_{org} values (~ 0.26) were found for smoldering-dominated combustion, while lower values (~ 0.1) were associated with flaming-dominated combustion. This indicates that OA from smoldering combustion is more hygroscopic, likely due to a higher degree of oxidation after prolonged aging. Therefore, the higher κ_{org} values observed in 2017 compared to 2016 may have contributed to the increased aerosol
450 hygroscopicity seen in 2017. However, since OA generally has lower hygroscopicity compared to inorganic aerosols, changes in κ_{org} alone may not fully explain the significant variation in κ between 2016 and 2017. Thus, changes in chemical composition caused by different burning conditions remain a critical factor in influencing overall aerosol hygroscopicity.

The decreased wind speed and increased RH in 2017 in the BB region over Africa suggest a reduction in the oxygen supply and a more humid atmosphere, which may have caused the BB to become more smoldering. Concurrently, sea surface wind
455 speeds around Ascension Island increased in 2017, potentially enhancing sea-salt aerosol emissions, which are rich in hygroscopic compounds like NaCl, thus increasing aerosol hygroscopicity observed during the 2017 BB season.

Overall, the changes in BB conditions appear to be the primary driver of the changes in aerosol hygroscopicity, which in turn affects CCN concentration and cloud properties. This underscores the important role of BB conditions on regional cloud properties and climate.

460 **Competing interests**

The contact author has declared that none of the authors has any competing interests.

Acknowledgment

The authors would like to thank the LASIC team, HC and MS gratefully acknowledge the funding of this research by the DOE-ASR grant DE-SC0020084. PZ gratefully acknowledges support from DOE-ASR grant DE-SC0021250. We thank Dr. Ernie
465 Lewis for his valuable discussions on the manuscript.

References

- Adebisi, A. A. and Zuidema, P.: The role of the southern African easterly jet in modifying the southeast Atlantic aerosol and cloud environments, *Quarterly Journal of the Royal Meteorological Society*, 142, 1574–1589, <https://doi.org/10.1002/qj.2765>, 2016.
- 470 Akagi, S. K., Craven, J. S., Taylor, J. W., McMeeking, G. R., Yokelson, R. J., Burling, I. R., Urbanski, S. P., Wold, C. E., Seinfeld, J. H., Coe, H., Alvarado, M. J., and Weise, D. R.: Evolution of trace gases and particles emitted by a chaparral fire in California, *Atmospheric Chemistry and Physics*, 12, 1397–1421, <https://doi.org/10.5194/acp-12-1397-2012>, 2012.



- Andreae, M. O. and Rosenfeld, D.: Aerosol–cloud–precipitation interactions. Part 1. The nature and sources of cloud-active aerosols, *Earth-Science Reviews*, 89, 13–41, <https://doi.org/10.1016/j.earscirev.2008.03.001>, 2008.
- 475 Boucher, O., Randall, D., Artaxo, P., Bretherton, C., Feingold, G., Forster, P., Kerminen, V.-M., Kondo, Y., Liao, H., Lohmann, U., Rasch, P., Satheesh, S. K., Sherwood, S., Stevens, B., and Zhang, X. Y.: Clouds and aerosols, in: *Climate Change 2013: The Physical Science Basis. Contribution of Working Group I to the Fifth Assessment Report of the Intergovernmental Panel on Climate Change*, edited by: Stocker, T. F., Qin, D., Plattner, G.-K., Tignor, M., Allen, S. K., Doschung, J., Nauels, A., Xia, Y., Bex, V., and Midgley, P. M., Cambridge University Press, Cambridge, UK, 571–657,
480 <https://doi.org/10.1017/CBO9781107415324.016>, 2013.
- Bougiatioti, A., Fountoukis, C., Kalivitis, N., Pandis, S. N., Nenes, A., and Mihalopoulos, N.: Cloud condensation nuclei measurements in the marine boundary layer of the Eastern Mediterranean: CCN closure and droplet growth kinetics, *Atmos. Chem. Phys.*, 9, 7053–7066, <https://doi.org/10.5194/acp-9-7053-2009>, 2009.
- Chang, R. Y.-W., Slowik, J. G., Shantz, N. C., Vlasenko, A., Liggio, J., Sjostedt, S. J., Leaitch, W. R., and Abbatt, J. P. D.:
485 The hygroscopicity parameter (κ) of ambient organic aerosol at a field site subject to biogenic and anthropogenic influences: relationship to degree of aerosol oxidation, *Atmos. Chem. Phys.*, 10, 5047–5064, <https://doi.org/10.5194/acp-10-5047-2010>, 2010.
- Che, H., Stier, P., Gordon, H., Watson-Parris, D., and Deaconu, L.: Cloud adjustments dominate the overall negative aerosol radiative effects of biomass burning aerosols in UKESM1 climate model simulations over the south-eastern Atlantic,
490 *Atmospheric Chemistry and Physics*, 21, 17–33, <https://doi.org/10.5194/acp-21-17-2021>, 2021.
- Che, H., Segal-Rozenhaimer, M., Zhang, L., Dang, C., Zuidema, P., Dobracki, A., Sedlacek, A. J., Coe, H., Wu, H., Taylor, J., Zhang, X., Redemann, J., and Haywood, J.: Cloud processing and weeklong ageing affect biomass burning aerosol properties over the south-eastern Atlantic, *Commun Earth Environ*, 3, 1–9, <https://doi.org/10.1038/s43247-022-00517-3>, 2022a.
- 495 Che, H., Segal-Rozenhaimer, M., Zhang, L., Dang, C., Zuidema, P., Sedlacek III, A. J., Zhang, X., and Flynn, C.: Seasonal variations in fire conditions are important drivers in the trend of aerosol optical properties over the south-eastern Atlantic, *Atmospheric Chemistry and Physics*, 22, 8767–8785, <https://doi.org/10.5194/acp-22-8767-2022>, 2022b.
- Che, H., Stier, P., Watson-Parris, D., Gordon, H., and Deaconu, L.: Source attribution of cloud condensation nuclei and their impact on stratocumulus clouds and radiation in the south-eastern Atlantic, *Atmospheric Chemistry and Physics Discussions*,
500 1–26, <https://doi.org/10.5194/acp-2022-43>, 2022c.
- Che, H. C., Zhang, X. Y., Zhang, L., Wang, Y. Q., Zhang, Y. M., Shen, X. J., Ma, Q. L., Sun, J. Y., and Zhong, J. T.: Prediction of size-resolved number concentration of cloud condensation nuclei and long-term measurements of their activation characteristics, *Sci Rep*, 7, <https://doi.org/10.1038/s41598-017-05998-3>, 2017.
- Christensen, M. W., Jones, W. K., and Stier, P.: Aerosols enhance cloud lifetime and brightness along the stratus-to-cumulus transition, *Proc Natl Acad Sci USA*, 117, 17591–17598, <https://doi.org/10.1073/pnas.1921231117>, 2020.
- 505 Conny, J. M. and Slater, J. F.: Black carbon and organic carbon in aerosol particles from crown fires in the Canadian boreal forest, *Journal of Geophysical Research: Atmospheres*, 107, AAC 4-1–AAC 4-12, <https://doi.org/10.1029/2001JD001528>, 2002.
- Dang, C., Segal-Rozenhaimer, M., Che, H., Zhang, L., Formenti, P., Taylor, J., Dobracki, A., Purdue, S., Wong, P.-S., Nenes, A., Sedlacek III, A., Coe, H., Redemann, J., Zuidema, P., Howell, S., and Haywood, J.: Biomass burning and marine aerosol
510

processing over the southeast Atlantic Ocean: a TEM single-particle analysis, *Atmospheric Chemistry and Physics*, 22, 9389–9412, <https://doi.org/10.5194/acp-22-9389-2022>, 2022.

515 Dedrick, J. L., Russell, L. M., Sedlacek III, A. J., Kuang, C., Zawadowicz, M. A., and Lubin, D.: Aerosol-Related Cloud Activation for Clean Conditions in the Tropical Atlantic Boundary Layer During LASIC, *Geophysical Research Letters*, 51, e2023GL105798, <https://doi.org/10.1029/2023GL105798>, 2024.

Dobracki, A., Lewis, E., Sedlacek III, A., Tatro, T., Zawadowicz, M., and Zuidema, P.: Burning conditions and transportation pathways determine biomass-burning aerosol properties in the Ascension Island marine boundary layer, *EGUsphere*, 1–51, <https://doi.org/10.5194/egusphere-2024-1347>, 2024.

520 Engelhart, G. J., Hennigan, C. J., Miracolo, M. A., Robinson, A. L., and Pandis, S. N.: Cloud condensation nuclei activity of fresh primary and aged biomass burning aerosol, *Atmospheric Chemistry and Physics*, 12, 7285–7293, <https://doi.org/10.5194/acp-12-7285-2012>, 2012.

Gordon, H., Field, P. R., Abel, S. J., Dalvi, M., Grosvenor, D. P., Hill, A. A., Johnson, B. T., Miltenberger, A. K., Yoshioka, M., and Carslaw, K. S.: Large simulated radiative effects of smoke in the south-east Atlantic, *Atmospheric Chemistry and Physics*, 18, 15261–15289, <https://doi.org/10.5194/acp-18-15261-2018>, 2018.

525 Han, S., Hong, J., Luo, Q., Xu, H., Tan, H., Wang, Q., Tao, J., Zhou, Y., Peng, L., He, Y., Shi, J., Ma, N., Cheng, Y., and Su, H.: Hygroscopicity of organic compounds as a function of organic functionality, water solubility, molecular weight and oxidation level, *Atmospheric Chemistry and Physics Discussions*, 1–26, <https://doi.org/10.5194/acp-2021-486>, 2021.

530 Haslett, S. L., Thomas, J. C., Morgan, W. T., Hadden, R., Liu, D., Allan, J. D., Williams, P. I., Keita, S., Lioussé, C., and Coe, H.: Highly controlled, reproducible measurements of aerosol emissions from combustion of a common African biofuel source, *Atmospheric Chemistry and Physics*, 18, 385–403, <https://doi.org/10.5194/acp-18-385-2018>, 2018.

535 Hersbach, H., Bell, B., Berrisford, P., Hirahara, S., Horányi, A., Muñoz-Sabater, J., Nicolas, J., Peubey, C., Radu, R., Schepers, D., Simmons, A., Soci, C., Abdalla, S., Abellan, X., Balsamo, G., Bechtold, P., Biavati, G., Bidlot, J., Bonavita, M., Chiara, G. D., Dahlgren, P., Dee, D., Diamantakis, M., Dragani, R., Flemming, J., Forbes, R., Fuentes, M., Geer, A., Haimberger, L., Healy, S., Hogan, R. J., Hólm, E., Janisková, M., Keeley, S., Laloyaux, P., Lopez, P., Lupu, C., Radnoti, G., Rosnay, P. de, Rozum, I., Vamborg, F., Villaume, S., and Thépaut, J.-N.: The ERA5 global reanalysis, *Quarterly Journal of the Royal Meteorological Society*, 146, 1999–2049, <https://doi.org/10.1002/qj.3803>, 2020.

540 Hodshire, A. L., Bian, Q., Ramnarine, E., Lonsdale, C. R., Alvarado, M. J., Kreidenweis, S. M., Jathar, S. H., and Pierce, J. R.: More Than Emissions and Chemistry: Fire Size, Dilution, and Background Aerosol Also Greatly Influence Near-Field Biomass Burning Aerosol Aging, *Journal of Geophysical Research: Atmospheres*, 124, 5589–5611, <https://doi.org/10.1029/2018JD029674>, 2019.

Kacarab, M., Thornhill, K. L., Dobracki, A., Howell, S. G., O'Brien, J. R., Freitag, S., Poellot, M. R., Wood, R., Zuidema, P., Redemann, J., and Nenes, A.: Biomass burning aerosol as a modulator of the droplet number in the southeast Atlantic region, *Atmospheric Chemistry and Physics*, 20, 3029–3040, <https://doi.org/10.5194/acp-20-3029-2020>, 2020.

545 Lu, Z., Liu, X., Zhang, Z., Zhao, C., Meyer, K., Rajapakshe, C., Wu, C., Yang, Z., and Penner, J. E.: Biomass smoke from southern Africa can significantly enhance the brightness of stratocumulus over the southeastern Atlantic Ocean, *PNAS*, 115, 2924–2929, <https://doi.org/10.1073/pnas.1713703115>, 2018.

Maßling, A., Wiedensohler, A., and Busch, B.: Hygroscopic properties of different aerosol types over the Atlantic and Indian Oceans, *Atmos. Chem. Phys.*, 21, 2003.



- 550 Ohata, S., Schwarz, J. P., Moteki, N., Koike, M., Takami, A., and Kondo, Y.: Hygroscopicity of materials internally mixed with black carbon measured in Tokyo, *Journal of Geophysical Research: Atmospheres*, 121, 362–381, <https://doi.org/10.1002/2015JD024153>, 2016.
- Petters, M. D. and Kreidenweis, S. M.: A single parameter representation of hygroscopic growth and cloud condensation nucleus activity, *Atmospheric Chemistry and Physics*, 7, 1961–1971, <https://doi.org/10.5194/acp-7-1961-2007>, 2007.
- 555 Pöhlker, M. L., Pöhlker, C., Quaas, J., Mülmenstädt, J., Pozzer, A., Andreae, M. O., Artaxo, P., Block, K., Coe, H., Ervens, B., Gallimore, P., Gaston, C. J., Gunthe, S. S., Henning, S., Herrmann, H., Krüger, O. O., McFiggans, G., Poulain, L., Raj, S. S., Reyes-Villegas, E., Royer, H. M., Walter, D., Wang, Y., and Pöschl, U.: Global organic and inorganic aerosol hygroscopicity and its effect on radiative forcing, *Nat Commun*, 14, 6139, <https://doi.org/10.1038/s41467-023-41695-8>, 2023.
- Prijith, S. S., Aloysius, M., and Mohan, M.: Relationship between wind speed and sea salt aerosol production: A new approach, *Journal of Atmospheric and Solar-Terrestrial Physics*, 108, 34–40, <https://doi.org/10.1016/j.jastp.2013.12.009>, 2014.
- 560 Ramanathan, V., Crutzen, P. J., Kiehl, J. T., and Rosenfeld, D.: Aerosols, Climate, and the Hydrological Cycle, *Science*, 294, 2119–2124, <https://doi.org/10.1126/science.1064034>, 2001.
- Redemann, J., Wood, R., Zuidema, P., Doherty, S. J., Luna, B., LeBlanc, S. E., Diamond, M. S., Shinozuka, Y., Chang, I. Y., Ueyama, R., Pfister, L., Ryoo, J.-M., Dobracki, A. N., da Silva, A. M., Longo, K. M., Kacenenbogen, M. S., Flynn, C. J., Pistone, K., Knox, N. M., Piketh, S. J., Haywood, J. M., Formenti, P., Mallet, M., Stier, P., Ackerman, A. S., Bauer, S. E., 565 Fridlind, A. M., Carmichael, G. R., Saide, P. E., Ferrada, G. A., Howell, S. G., Freitag, S., Cairns, B., Holben, B. N., Knobelspiesse, K. D., Tanelli, S., L’Ecuyer, T. S., Dzambo, A. M., Sy, O. O., McFarquhar, G. M., Poellot, M. R., Gupta, S., O’Brien, J. R., Nenes, A., Kacarab, M., Wong, J. P. S., Small-Griswold, J. D., Thornhill, K. L., Noone, D., Podolske, J. R., Schmidt, K. S., Pilewskie, P., Chen, H., Cochrane, S. P., Sedlacek, A. J., Lang, T. J., Stith, E., Segal-Rozenhaimer, M., Ferrare, R. A., Burton, S. P., Hostetler, C. A., Diner, D. J., Seidel, F. C., Platnick, S. E., Myers, J. S., Meyer, K. G., Spangenberg, D. 570 A., Maring, H., and Gao, L.: An overview of the ORACLES (ObseRvations of Aerosols above CLouds and their intERactionS) project: aerosol–cloud–radiation interactions in the southeast Atlantic basin, *Atmospheric Chemistry and Physics*, 21, 1507–1563, <https://doi.org/10.5194/acp-21-1507-2021>, 2021.
- Roberts, G. C. and Nenes, A.: A Continuous-Flow Streamwise Thermal-Gradient CCN Chamber for Atmospheric Measurements, *Aerosol Science and Technology*, 39, 206–221, <https://doi.org/10.1080/027868290913988>, 2005.
- 575 Rose, D., Nowak, A., Achtert, P., Wiedensohler, A., Hu, M., Shao, M., Zhang, Y., Andreae, M. O., and Pöschl, U.: Cloud condensation nuclei in polluted air and biomass burning smoke near the mega-city Guangzhou, China – Part 1: Size-resolved measurements and implications for the modeling of aerosol particle hygroscopicity and CCN activity, *Atmospheric Chemistry and Physics*, 10, 3365–3383, <https://doi.org/10.5194/acp-10-3365-2010>, 2010.
- 580 Rose, D., Gunthe, S. S., Su, H., Garland, R. M., Yang, H., Berghof, M., Cheng, Y. F., Wehner, B., Achtert, P., Nowak, A., Wiedensohler, A., Takegawa, N., Kondo, Y., Hu, M., Zhang, Y., Andreae, M. O., and Pöschl, U.: Cloud condensation nuclei in polluted air and biomass burning smoke near the mega-city Guangzhou, China -Part 2: Size-resolved aerosol chemical composition, diurnal cycles, and externally mixed weakly CCN-active soot particles, *Atmospheric Chemistry and Physics*, 11, 2817–2836, <https://doi.org/10.5194/acp-11-2817-2011>, 2011.
- 585 Rosenfeld, D., Lohmann, U., Raga, G. B., O’Dowd, C. D., Kulmala, M., Fuzzi, S., Reissell, A., and Andreae, M. O.: Flood or drought: How do aerosols affect precipitation?, *Science*, 321, 1309–1313, <https://doi.org/10.1126/science.1160606>, 2008.
- Sanchez-Marroquin, A., Hedges, D. H. P., Hiscock, M., Parker, S. T., Rosenberg, P. D., Trembath, J., Walshaw, R., Burke, I. T., McQuaid, J. B., and Murray, B. J.: Characterisation of the filter inlet system on the FAAM BAe-146 research aircraft and



- its use for size-resolved aerosol composition measurements, *Atmospheric Measurement Techniques*, 12, 5741–5763, <https://doi.org/10.5194/amt-12-5741-2019>, 2019.
- 590 Santoso, M. A., Christensen, E. G., Yang, J., and Rein, G.: Review of the Transition From Smouldering to Flaming Combustion in Wildfires, *Front. Mech. Eng.*, 0, <https://doi.org/10.3389/fmech.2019.00049>, 2019.
- Schulze, B. C., Charan, S. M., Kenseth, C. M., Kong, W., Bates, K. H., Williams, W., Metcalf, A. R., Jonsson, H. H., Woods, R., Sorooshian, A., Flagan, R. C., and Seinfeld, J. H.: Characterization of Aerosol Hygroscopicity Over the Northeast Pacific Ocean: Impacts on Prediction of CCN and Stratocumulus Cloud Droplet Number Concentrations, *Earth and Space Science*, 7, e2020EA001098, <https://doi.org/10.1029/2020EA001098>, 2020.
- 595 Sedlacek, A. J. I., Lewis, E. R., Onasch, T. B., Zuidema, P., Redemann, J., Jaffe, D., and Kleinman, L. I.: Using the Black Carbon Particle Mixing State to Characterize the Lifecycle of Biomass Burning Aerosols, *Environ. Sci. Technol.*, 56, 14315–14325, <https://doi.org/10.1021/acs.est.2c03851>, 2022.
- Seinfeld, J. H. and Pandis, S. N.: *Atmospheric Chemistry and Physics: From Air Pollution to Climate Change*, John Wiley & Sons, 1146 pp., 2016.
- 600 Soden, B. J. and Vecchi, G. A.: The vertical distribution of cloud feedback in coupled ocean-atmosphere models, *Geophysical Research Letters*, 38, <https://doi.org/10.1029/2011GL047632>, 2011.
- Weimer, S., Alfarra, M. R., Schreiber, D., Mohr, M., Prévôt, A. S. H., and Baltensperger, U.: Organic aerosol mass spectral signatures from wood-burning emissions: Influence of burning conditions and wood type, *Journal of Geophysical Research: Atmospheres*, 113, <https://doi.org/10.1029/2007JD009309>, 2008.
- 605 Wilcox, E. M.: Direct and semi-direct radiative forcing of smoke aerosols over clouds, *Atmospheric Chemistry and Physics*, 12, 139–149, <https://doi.org/10.5194/acp-12-139-2012>, 2012.
- Wood, R.: Stratocumulus Clouds, *Mon. Wea. Rev.*, 140, 2373–2423, <https://doi.org/10.1175/MWR-D-11-00121.1>, 2012.
- Zhang, L., Segal-Rozenhaimer, M., Che, H., Dang, C., Sun, J., Kuang, Y., Formenti, P., and Howell, S.: Aerosol hygroscopicity over the South-East Atlantic Ocean during the biomass burning season: Part I – From the perspective of scattering enhancement, *EGUsphere*, 1–34, <https://doi.org/10.5194/egusphere-2023-2199>, 2023.
- 610 Zheng, B., Chevallier, F., Ciaï, P., Yin, Y., and Wang, Y.: On the Role of the Flaming to Smoldering Transition in the Seasonal Cycle of African Fire Emissions, *Geophysical Research Letters*, 45, 11,998–12,007, <https://doi.org/10.1029/2018GL079092>, 2018.
- 615 Zuidema, P., Alvarado, M., Chiu, C., DeSzoëke, S., Fairall, C., Feingold, G., Freedman, A., Ghan, S., Haywood, J., Kollias, P., Lewis, E., McFarquhar, G., McComiskey, A., Mechem, D., Onasch, T., Redemann, J., Romps, D., and Turner, D.: Layered Atlantic Smoke Interactions with Clouds (LASIC) Field Campaign Report, 47, 2018a.
- Zuidema, P., Sedlacek, A. J., Flynn, C., Springston, S., Delgadoillo, R., Zhang, J., Aiken, A. C., Koontz, A., and Muradyan, P.: The Ascension Island Boundary Layer in the Remote Southeast Atlantic is Often Smoky, *Geophysical Research Letters*, 45, 4456–4465, <https://doi.org/10.1002/2017GL076926>, 2018b.
- 620